0888-8809/05/$15.00/0
Printed in U.S.A.

Molecular Endocrinology 19(3):698–710

doi: 10.1210/me.2004-0341

Role of PROP1 in Pituitary Gland Growth

Robert D. Ward, Lori T. Raetzman, Hoonkyo Suh, Brandon M. Stone, Igor O. Nasonkin, and Sally A. Camper

Graduate Program in Cellular and Molecular Biology (R.D.W., S.A.C.), Department of Human Genetics (L.T.R., B.M.S., I.O.N., S.A.C.), Graduate Program in Neuroscience (H.S.), University of Michigan, Ann Arbor, Michigan 48109-0638

Mutations in the *PROP1* transcription factor gene lead to reduced production of thyrotropin, GH, prolactin, and gonadotropins as well as to pituitary hypoplasia in adult humans and mice. Some *PROP1*-deficient patients initially exhibit pituitary hyperplasia that resolves to hypoplasia. To understand this feature and to explore the mechanism whereby PROP1 regulates anterior pituitary gland growth, we carried out longitudinal studies in normal and *Prop1*-deficient dwarf mice from early embryogenesis through adulthood, examining the volume of Rathke's pouch and its derivatives, the position and number of dividing cells, the rate of apoptosis, and cell migration by pulse labeling. The results suggest that anterior pituitary progenitors normally leave the perilumenal region of Rathke's pouch and migrate to form the anterior lobe as they differentiate. Some of the cells that seed the anterior lobe during organogenesis have proliferative potential, supporting the expansion of the anterior lobe after birth. *Prop1*-deficient fetal pituitaries are dysmorphic because mutant cells are retained in the perilumenal area and fail to differentiate. After birth, mutant pituitaries exhibit enhanced apoptosis and reduced proliferation, apparently because the mutant anterior lobe is not seeded with progenitors. These studies suggest a mechanism for *Prop1* action and an explanation for some of the clinical findings in human patients. (*Molecular Endocrinology* 19: 698–710, 2005)

APPROXIMATELY 1:4000 live births result in pituitary growth insufficiency (1, 2). Isolated GH deficiency is the most common and is often caused by deletions within the GH gene cluster (3, 4). Combined pituitary hormone deficiency (CPHD) is defined as a deficiency in GH and at least one other hormone, and it is caused by a variety of transcription factor mutations. The majority of CPHD cases of known cause result from mutations in the transcription factors, *PROP1* and *POU1F1*(*PIT1*), whereas mutations in *HESX1*, *LHX3*, and *LHX4* are more rare and are associated with additional structural anomalies (5–12). Mutations in *PIT1* produce deficiencies in GH, prolactin (PRL), and TSH (13). *PROP1* mutations cause deficiencies in the same hormones as *PIT1*, with additional reductions in LH and FSH, as well as acquired ACTH loss (14–16). Affected individuals exhibit a high level of variation in the age of onset and the severity of the disease. The hormone deficiencies are progressive and can occur in childhood or later in life (17, 18). Particularly intriguing is the observation that many patients with *PROP1* mutation undergo apparent degeneration of the pituitary gland during childhood (19). Initially, magnetic resonance imaging analysis reveals a hyperplastic, or enlarged, pituitary gland, which resolves to a hypoplastic appearance a year or so later. The progressive hormone loss and pituitary degeneration are exclusively associated with *PROP1* mutations.

Two mouse models are available for dissecting the mechanism of PROP1 action: the spontaneous mutant known as Ames dwarf (*Prop1*^{df}) and the genetically engineered *Prop1*^{null} mouse (20, 21). Both models have hormone deficiencies that recapitulate the human CPHD phenotype, including reduced gonadotropins; lack of TSH, GH, and PRL; and profound adult pituitary hypoplasia (21, 22). Although some evidence suggests that the missense mutation in Ames dwarf mice is a hypomorphic allele, the phenotypes of the *df* and null alleles are virtually indistinguishable when compared on the same genetic background (21). Previous studies have elucidated some aspects of *Prop1* action. For example, the TSH, GH, and PRL deficiencies result from the failure to activate *Pit1* transcription, which is essential for the lineage of cells that produce these hormones (23, 24). The nature of the gonadotropin deficiency is less obvious (25). For example, the gonadotrope-specific transcription factor SF1 (*Nr5a1*) is overexpressed in the absence of *Prop1* (26), and gonadotropin production can be induced in *Prop1*-deficient mice by correction of the GH and TSH deficiencies, suggesting adequate commitment to the gonadotrope fate (27). The mutant mice exhibit a delay in gonadotrope differentiation on some genetic back-

First Published Online December 9, 2004

Abbreviations: BrdU, Bromodeoxyuridine; CPHD, combined pituitary hormone deficiency; DAPI, 4,6-diamidino-2-phenylindole, dihydrochloride; FGF, fibroblast growth factor; FITC, fluorescein isothiocyanate; H&E, hematoxylin and eosin; IdU, iododeoxyuridine; POMC, proopiomelanocortin; PRL, prolactin; TRITC, tetramethyl rhodamine isothiocyanate; TUNEL, terminal deoxynucleotidyl transferase-mediated deoxyuridine triphosphate nick end labeling.

***Molecular Endocrinology* is published monthly by The Endocrine Society (http://www.endo-society.org), the foremost professional society serving the endocrine community.**

grounds, however, which supports the hypothesis that gonadotropes fail to develop in humans with *PROP1* mutations (21).

One aspect of the mouse *Prop1*-deficient phenotype that remains unexplained is the profound dysmorphology of the dorsal aspect of Rathke's pouch at embryonic d 14.5 (e14.5) (20, 22). Pituitary development begins at approximately e9 in the mouse, with a thickening of the oral ectoderm to form the pituitary placode, which grows and invaginates to produce Rathke's pouch and eventually becomes the intermediate and anterior lobes of the pituitary gland. Rathke's pouch is in direct contact with the neural ectoderm of the ventral diencephalon, which evaginates to form the infundibulum, ultimately becoming the posterior lobe of the pituitary gland and pituitary stalk (28, 29). By e12.5, Rathke's pouch has become separated from the oral ectoderm and has begun to expand to form the anterior lobe. The growth and shape of the pouch is influenced by factors secreted from the infundibulum, such as fibroblast growth factor (FGF)8, FGF10, bone morphogenetic protein 4, and WNT5A, some of which are regulated by *Sox3* expression (30–34). At e12.5, the proliferating cells within the pituitary primordium are almost exclusively located in the perilumenal area, with the highest rate of proliferation at the dorsal tip of Rathke's pouch (35, 36). There are few or no proliferating cells in the developing anterior lobe at this time, which suggests that quiescent cells normally stream out of the pouch and populate the developing anterior lobe. At e12.5, *Prop1*-deficient pituitaries are indistinguishable from wild type in shape, cell proliferation, and cell death (36). By e14.5, however, the mutant anterior lobes are 50% smaller than wild type and the dorsal aspect of Rathke's pouch appears overgrown and dysmorphic (22). The dorsal overgrowth of Rathke's pouch in *Prop1* mutants is hypothesized to be equivalent to the initial hyperplasia of the pituitaries of *PROP1*-deficient patients, but there have been no longitudinal studies of pituitary gland growth in *Prop1* mutant mice (37).

In this study, we compare pituitary growth in the *Prop1*-deficient and wild-type mice. *Prop1* expression begins at about e10 in the mouse, peaks at e12.5, and essentially ceases by e16 (20). Surprisingly, the size of the organ primordia is indistinguishable in mutant and wild-type mice during this time. Instead, overall hypoplasia first becomes obvious long after the time in which *Prop1* is normally expressed, becoming significant around 2 wk of age and accompanied by enhanced cell death and reduced proliferation. We show that proliferating cells normally migrate from the pouch into the developing anterior lobe, and this process is impaired in *Prop1* mutant mice. Mutant progenitors cease expression of cyclin D2 but retain tight contact with neighboring cells and do not seed the anterior lobe, ultimately resulting in profound hypoplasia of the organ. This study provides basic information about how the pituitary gland forms and enhances our understanding of the mechanism of PROP1 action. Furthermore, our studies provide a plausible explanation for the intriguing transition from hyperplasia to hypoplasia in humans with *PROP1* mutations.

RESULTS

Prop1 Deficiency Results in Pituitary Dysmorphology

The Ames dwarf (*Prop1*^{df}) pituitary is dysmorphic and has an underdeveloped anterior lobe that is approximately 50% smaller than normal at e14 (22). By 8 wk, the adult *Prop1*$^{df/df}$ organ is about 7-fold smaller than normal by weight, indicative of severe hypoplasia (38). There is no difference, however, in the location or quantity of proliferating or dying cells in wild-type and dwarf pituitaries at e12.5 or e14.5 (36). To determine the effect of *Prop1* deficiency on the growth and shape of the pituitary throughout development and early postnatal life, timed pregnancies were generated with *Prop1*$^{df/+}$ heterozygote matings. Fetuses were collected at e14.5 and e17.5 and processed for histology. Serial sections cut coronally and stained with hematoxylin and eosin (H&E) confirm that the anterior lobe of the pituitary has started to develop in normal mice at e14.5 (Fig. 1A). The anterior lobe continues to grow laterally throughout embryonic (Fig. 1C) and postnatal development (Fig. 1E). In *Prop1*$^{df/df}$ mice, the anterior lobe is smaller than normal at e14.5, but Rathke's pouch has expanded abnormally and the lumen is much larger than wild type (Fig. 1B). By e17.5, the mutant perilumenal cells have continued to expand, growing dorsally and nearly covering the posterior lobe (Fig. 1D). The lumen is collapsed, presumably because of the overgrowth, resulting in the extremely dysmorphic pituitary primordium characteristic of *Prop1*$^{df/df}$ mice. The overall size of normal and dwarf pituitaries appears similar at e17.5, despite the minute anterior lobe in mutants. At postnatal d 8 (P8), the dysmorphology remains prominent in dwarfs, and the overall growth of the dwarf pituitary appears to have fallen behind that of the wild type (Fig. 1F).

Volumetric Analysis Confirms Growth Defect in *Prop1*-Deficient Pituitaries after Birth

The volume of the Rathke's pouch and its derivatives was quantitated by computerized, three-dimensional reconstruction from serial sections of wild-type and Ames dwarf pituitaries from e12.5 through adulthood (8 wk). A computer program was used to calculate the total anterior and intermediate lobe volume of each pituitary, and the results from several individuals of the same genotype were averaged (Fig. 1G). Although the *Prop1*$^{df/df}$ e14.5 pituitary gland appears larger than the wild type when comparing H&E-stained sections, there is no difference in the volume of wild-type and *Prop1*$^{df/df}$ pituitaries at e14.5 when corrected for the expanded lumen volume, suggesting that the total

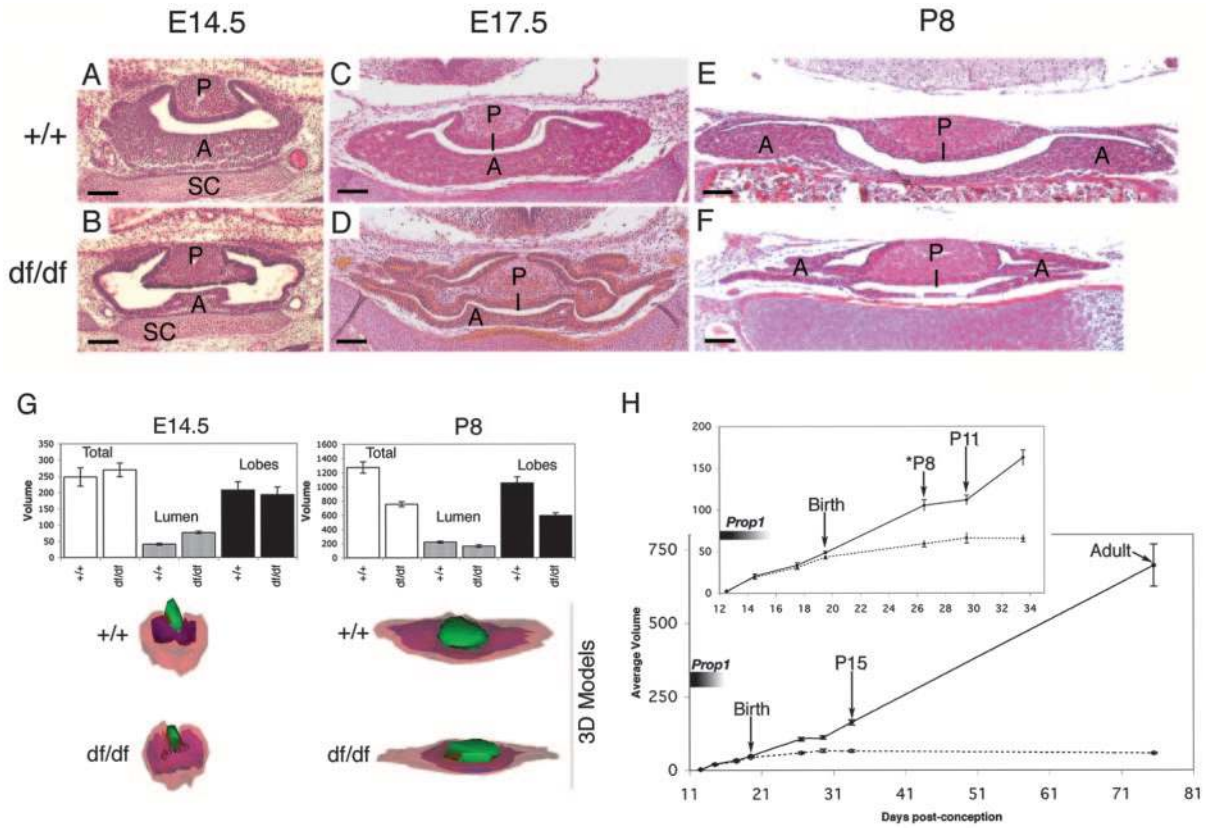

Fig. 1. Dysmorphology of *Prop1*$^{df/df}$ Pituitaries is Evident during Gestation and Overall Hypoplasia is Prominent after Birth

Prop1$^{+/+}$ (A, C, and E) and *Prop1*$^{df/df}$ (B, D, and F) embryos and neonates were sectioned in the coronal plain and stained with H&E to examine the pituitary morphology at e14.5 (A and B), e17.5 (C and D), and P8 (E and F). *Prop1*-deficient mice (B) have an expanded lumen relative to wild type (A) that eventually folds over on itself by e17.5, giving the mutant organ a profoundly dysmorphic appearance (D) compared with wild type (C). By P8, the *Prop1*$^{df/df}$ pituitary, including both prospective anterior and intermediate lobes, is hypoplastic and dysmorphic (F), relative to wild type mice (E). P, Posterior lobe; I, intermediate lobe; A, anterior lobe; SC, sphenoid cartilage. *Scale bar*, 100μm. G, The average volume of the prospective anterior and intermediate lobes (*black bars*) of *Prop1*$^{+/+}$ and *Prop1*$^{df/df}$ mice is calculated in 10^4 μm^3 by subtracting the volume of the lumen (*gray bars*) from the total organ displacement (*white bars*) at e14.5 (*left*; n = 3 +/+ and 4 df/df) and P8 (*right*; n =5 +/+ and 3 df/df). There is no statistical difference in the average pituitary volume of wild-type and mutant mice at e14.5 ($P > 0.05$), but the cellular volume of the *Prop1*$^{df/df}$ pituitary is 1.8-fold smaller than wild type at P8 ($P < 0.005$). Three-dimensional models of wild-type and *Prop1*$^{df/df}$ pituitaries at e14.5 (*left*) and P8 (*right*) illustrate the anterior and intermediate lobes (*pink*), the lumen (*red*), and the posterior lobe (*green*). H, Average volumes of Rathke's pouch derivatives in *Prop1*-deficient mice (*dotted line*) are the same as wild type (*solid line*) until birth. After birth, the *Prop1*$^{df/df}$ pituitaries fail to grow and are 60% smaller than wild type by P8; *, $P < 0.005$. There is no statistical difference in the volume of adult and P8 *Prop1*$^{df/df}$ pituitaries; *, $P > 0.5$. The *black bar* shows *Prop1* expression in normal mice. The number of mice analyzed at each time point is as follows (n = +/+ and df/df): e12.5, n = 3 and 3; e14.5, n = 3 and 4; e17.5, n = 3 and 3; P1, n = 3 and 3; P8, n = 5 and 3; P11, n = 5 and 4; P15, n = 3 and 4; adult, n = 3 and 3. *Y-axis scale*, 100,000 μm^3.

number of cells is similar (Fig. 1G, *top left*). The overall size and shape of Rathke's pouch derivatives can be appreciated in three-dimensional images typical of mutant and wild-type mice (Fig. 1G, *bottom left*). This is consistent with the evidence for identical cell proliferation and cell death rates at this time (36). In contrast, by 1 wk of age, the overall volume of the dwarf pituitary is approximately 1.8-fold smaller that of the wild type (Fig. 1G, *right*). The smaller volume is also evident in three-dimensional reconstruction.

The growth of wild-type and *Prop1*$^{df/df}$ pituitaries was quantified throughout development, starting at e12.5 and proceeding through 8 wk of postnatal development (Fig. 1H). No significant differences were found in the combined volumes of the anterior and intermediate lobes of mutant and wild type at e12.5, e14.5, e17.5, or on the day of birth. The volume of wild-type and the *Prop1*$^{df/df}$ pituitaries differed significantly at P8 and P11, and the differences became even more pronounced at P15. Apparently the dwarf pituitary almost completely ceases growing after birth, even though the body weight of the animal continues to increase until adulthood (21). By 8 wk, a drastic, 10-fold difference in dwarf and normal pituitary volume is evident, consistent with the approximate pituitary weight difference previously reported for adult mice (38).

Proliferating Cells Fail to Populate the Anterior Lobe of *Prop1*-Deficient Mice

The volumetric measurements suggest that proliferation and/or cell death rates are likely to be altered in *Prop1*$^{df/df}$ mice after birth, after *Prop1* expression has waned. To determine whether this is the case, we examined cell proliferation by injecting pregnant dams and neonates with the thymidine analog bromodeoxyuridine (BrdU), which is incorporated into replicating DNA and is detectable by immunohistochemistry. At e14.5, the vast majority of proliferating cells surround the lumen and posterior lobe in wild-type mice (Fig. 2, A and A′). Very few proliferating cells are within the developing anterior lobe. By e17.5, a large portion of the proliferating cells appear in the expanding anterior lobe, although there are still proliferating cells surrounding the lumen (Fig. 2, C and C′). By P8, the majority of the proliferating cells are detected in the anterior lobe (Fig. 2, E and E′). In Ames dwarf mice, proliferating cells line the lumen at e14.5, similar to the pattern characteristic of normal pituitaries (Fig. 2, B and B′). At e17.5, there are fewer dividing cells in anterior lobes of mutants than wild types (Fig. 2, D and D′). At P8, this difference is even more pronounced (Fig. 2, F and F′). This lack in proliferation of the dwarf anterior lobe is evident at P11 and P15 (data not shown), which is consistent with the reduced pituitary volume of mutants relative to wild type at this time.

Cyclin D2 is expressed during the G1 phase of the cell cycle and is essential for the passage of the cell into S phase (40). At e14.5, cyclin D2 is expressed exclusively in the proliferative zone of wild-type pituitaries (Fig. 3B). In Ames dwarfs, cyclin D2-positive cells are also detected in the proliferative zone (Fig. 3F), but there appear to be fewer of them than normal. In addition, the cyclin D2-positive cells appear to be interspersed with cyclin D2-negative cells in the dwarf, suggesting that the actively dividing cells in mutants are interdigitated with quiescent cells. Ki67 is expressed in cells that are actively cycling (41). Ki67 is expressed in the proliferative zone of both wild-type and dwarf pituitaries (Fig. 3, C and G). The dwarf pituitary exhibited fewer Ki67-positive cells, indicating an increase in quiescent cells (Fig. 3G). In the wild type, the vast majority of Ki67+ cells are also positive for cyclin D2 (Fig. 3D, *yellow cells*). There are only a few Ki67-positive, cyclin D2-negative cells surrounding the proliferative zone of the wild-type pituitaries (Fig. 3D, *green*, *arrowheads/inset*), which suggests that the vast majority of actively dividing cells are exiting G1 and entering S phase rapidly. In the dwarf, however, there is an approximate 3-fold increase in Ki67-positive, cyclin D2-negative cells in the pouch (Fig. 3H, *green*, *arrowheads/inset*), suggesting that some of the mutant cells are stalled in G1 phase in addition to being interspersed with more quiescent cells. The cyclin D2 and Ki67 immunostaining results

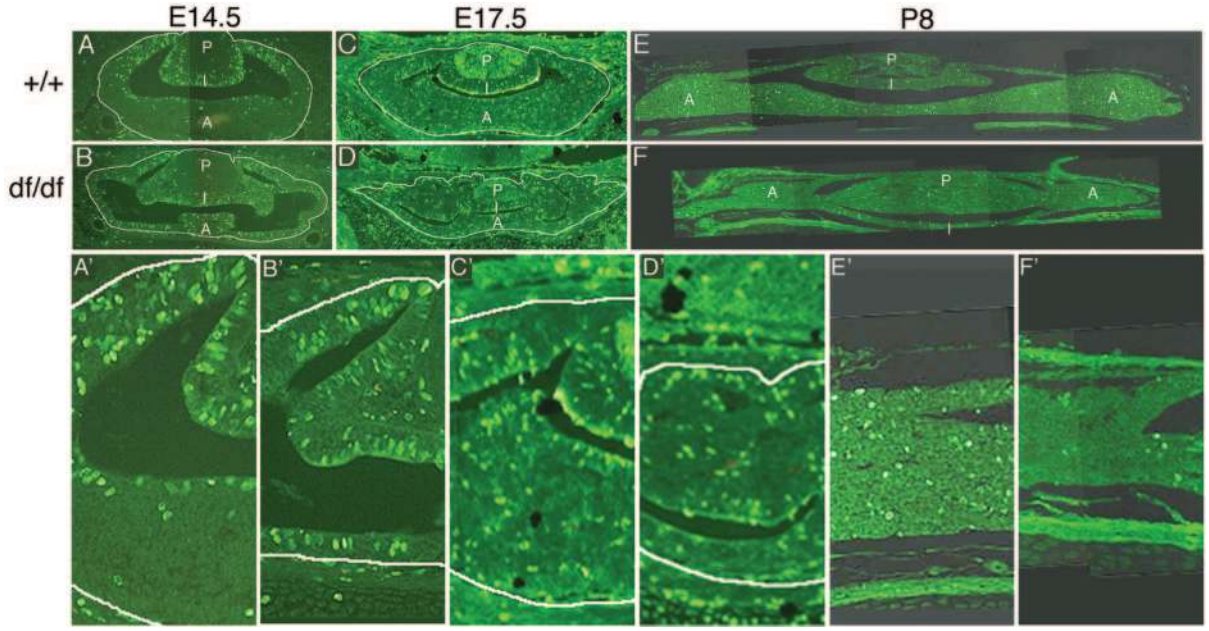

Fig. 2. Progenitors Fail to Populate the Anterior Lobe of *Prop1*$^{df/df}$ Pituitaries, Resulting in Decreased Proliferation after Birth

Immunostaining of BrdU-injected embryos and neonates was performed to assess proliferation levels and patterns at e14.5 (A and B), e17.5 (C and D), and P8 (E and F). Proliferating cells (*bright green*) surround the lumen and are absent from the anterior lobe in both the wild-type (A and A′) and *Prop1*$^{df/df}$ (B and B′) pituitaries at e14.5. Proliferating cells are detectable in both the perilumenal area and the anterior lobe of wild type-mice at e17.5 (C and C′). The *Prop1*$^{df/df}$ pituitary has an extremely small anterior lobe at e17.5 (D and D′). By P8, the *Prop1*$^{df/df}$ pituitary (F and F′) has fewer proliferating cells in the expanding anterior lobe than the wild type (E and E′). P, Posterior lobe; I, intermediate lobe; A, anterior lobe. Original magnification, ×200 (A and B), ×100 (C–F).

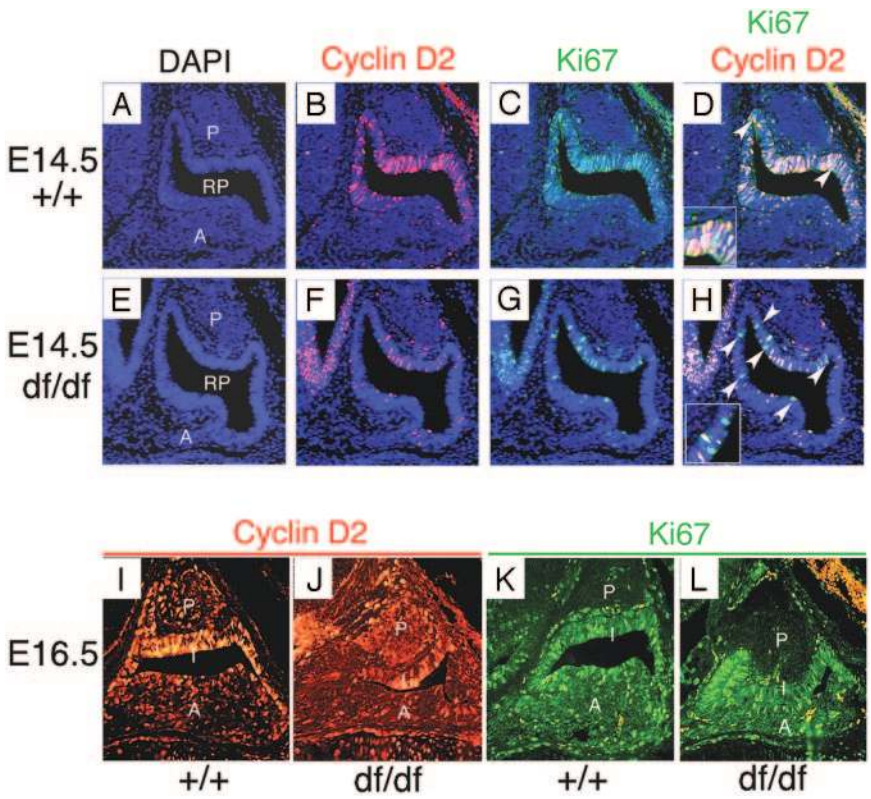

Fig. 3. Cell Cycle Differences between Wild-Type and *Prop1*$^{df/df}$ Pituitaries

Cell cycle marker expression was examined in e14.5 wild-type (A–D), e14.5 dwarf (E–H), e16.5 wild-type (I and K), and e16.5 dwarf (J and L) pituitaries. DAPI (*blue*) counterstain in e14.5 wild-type (A) and dwarf (E) pituitaries. At e14.5, cyclin D2 (*red*) expression in wild-type (B) *vs.* dwarf (F) and Ki67 (*green*) expression in wild-type (C) *vs.* dwarf (G) pituitaries reveals an increase in noncycling cells in the proliferative zone of the dwarf pituitary. Cyclin D2/Ki67 colocalization (*yellow*) *vs.* Ki67 only (*green*, *arrowheads/insets*) expression in wild-type (D) and dwarf (H) pituitaries at e14.5 reveal an increase in cycling cells that remain in G1 phase of the cell cycle in the dwarf pituitary. Analysis of pituitaries at e16.5 shows a decrease in cyclin D2-positive cells (*red*) in the dwarf proliferative zone (J) compared with the wild type (I), whereas Ki67 expression (*green*) appears the same in both the wild type (K) and the dwarf (L) at this time. The structure to the *left of the dwarf pituitary* (E–H) is the ventral diencephalon, which is not seen in the wild-type pituitary picture shown (A–D). This is due only to the slight differences in the plane of the section and is not specific to the mutant. P, Posterior lobe; RP, Rathke's pouch; I, intermediate lobe; A, anterior lobe. The number of pituitary sections analyzed for each time point is as follows (n = +/+ and df/df): e14.5, n = 7 and 10; e16.5, n = 3 and 3. Original magnification, ×200.

suggest that mutant cells leave the cell cycle but remain in the proliferative zone instead of populating the anterior lobe. At e16.5, cyclin D2 expression is reduced considerably in the dwarf (Fig. 3J) compared with the wild type (Fig. 3I), although the Ki67 expression is similar in both (compare Fig. 3L with 3K). This data suggests that the cell cycle defect that was seen at e14.5 persists at later times in embryonic development, as cells are apparently stalled in the G1 phase of the cell cycle in dwarf pituitaries.

Prop1$^{df/df}$ Pituitaries Exhibit a Progenitor Migration Defect

We hypothesize that the dividing cells located in the proliferative zone at e12.5 temporarily cease cell division as they stream into the anterior lobe at e14.5 in normal mice. Furthermore, we propose that the *Prop1* defect causes reduced progenitor migration that results in both the dorsal dysmorphology and ventral hypoplasia of the mutant anterior lobe at e14.5. To test these ideas, we examined the migration patterns of dividing cells during the period of peak *Prop1* expression using pulse chase labeling of growing DNA chains with the nucleoside analogs iododeoxyuridine (IdU) and BrdU. IdU and BrdU are similar thymidine analogs, but, after incorporation into replicating DNA, they can be distinguished by immunohistochemistry. Unincorporated nucleoside analogs are cleared within 2 h after injection (42, 43). Thus, the "chase" does not require injection of normal, unmarked nucleosides, and fetuses collected several days after the chase reveal the ultimate location of cells proliferating during the pulse. This window labeling method, involving sequential injections of IdU and BrdU at different times of development, has proved valuable for demonstrating cell migration patterns in other organs (44).

We labeled cells during the S phase of the cell cycle at e11.5 (Fig. 4A) and e12.5 (Fig. 4B) with IdU and BrdU, respectively, and collected fetuses at e14.5 (Fig. 4C) to determine the destination of the previously proliferating cells. According to our hypothesis, a portion of the cells proliferating at e11.5 (IdU labeled) will have migrated into the anterior lobe by e12.5 in both normal and *Prop1*-deficient mice, whereas cells proliferating at e12.5 (BrdU labeled), the peak time of *Prop1* expression, will be compromised in their ability to populate the anterior lobe in *Prop1* mutants. At e14.5 the cells of the anterior pituitary lobe are somewhat intermingled with the surrounding mesenchymal tissue, so we used the PITX1 antibody to mark the pituitary cells unequivocally. The IdU antibody detects both the IdU and BrdU analogs. Therefore, cells that were labeled at e11.5 with IdU and e12.5 with BrdU will appear *red* when visualized with the IdU antibody and tetramethyl rhodamine isothiocyanate (TRITC) fluorescence (Fig. 4D). Cells that were labeled with BrdU at e12.5 appear *green* when visualized with the BrdU-specific antibody and fluorescein isothiocyanate (FITC) fluorescence (Fig. 4E). When the FITC and TRITC images are overlayed, the BrdU-labeled cells appear *yellow* as a result of the combination of the red and green fluorescence, whereas the IdU labeled cells appear *red* (Fig. 4F).

In the pituitaries of normal mice, cells that were labeled at e11.5 and e12.5 populate both the anterior lobe and the perilumenal area at e14.5, although the majority are in the anterior lobe (Fig. 4, D–F). This provides the first compelling evidence that the anterior lobe normally forms by movement of cells from the

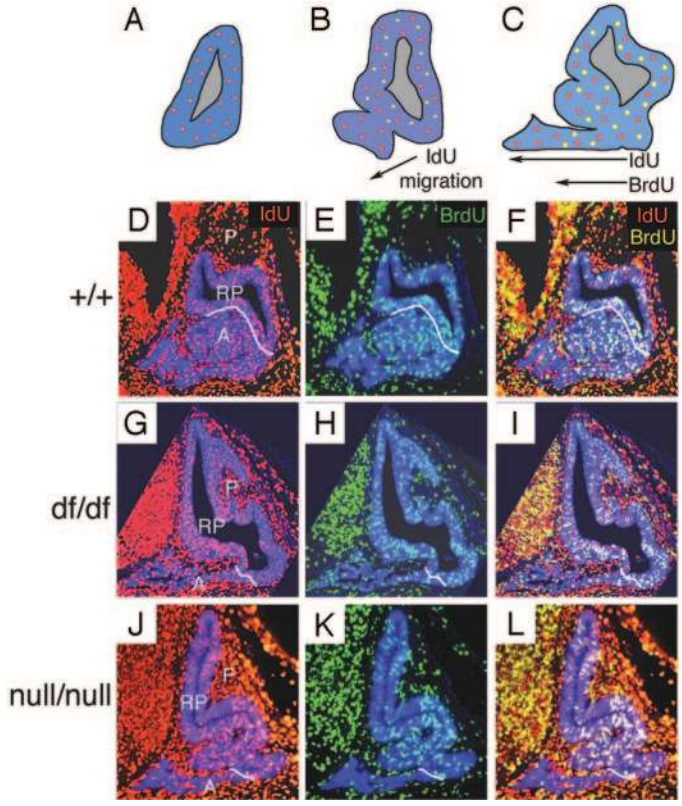

Fig. 4. *Prop1*^{null} Pituitaries Exhibit Migratory Defects during Embryonic Development

A–C, Schematic representation of the IdU/BrdU pulse-chase experiment. A, IdU is injected at e11.5 and incorporated into the DNA of proliferating cells (visualized as *red dots*). Rathke's pouch and its derivatives are marked by PITX1 immunohistochemical staining (*blue*). B, BrdU is injected at e12.5 (visualized as *yellow dots*). At this time, the IdU-positive cells in the developing anterior lobe must have actively or passively moved there. C, BrdU-positive cells follow the IdU-labeled cells into the developing anterior lobe. Embryos are harvested at e14.5. The pulse-chase experiment was carried out for wild-type (D–F), *Prop1*$^{df/df}$ (G–I), and *Prop1*$^{null/null}$ (J–L) animals. D, G, and J, TRITC images of the IdU- and BrdU-labeled cells (*red*) because the IdU antibody recognized both the IdU- and BrdU-incorporated analogs. At e14.5, cells that were injected with IdU at e11.5 have reached the anterior lobe in the wild-type (D), *Prop1*$^{df/df}$ (G), and *Prop1*$^{null/null}$ (J) animals. E, H, and K, FITC images of the BrdU-only-labeled cells (*green*). The cells that were labeled with BrdU at e12.5 were plentiful in the anterior lobe of the wild type (E) with an even distribution between the proliferative zone and the anterior lobe. The *Prop1*$^{df/df}$ e14.5 pituitary revealed the majority of the BrdU-labeled cells remaining in the dysmorphic, perilumenal area (H). The *Prop1*$^{null/null}$ pituitary showed very few BrdU-labeled cells in the anterior lobe (K). F, I, and L, Overlays of the TRITC and FITC images. The IdU-only-labeled cells appear *red*, whereas the BrdU-labeled cells appear *yellow* as a result of the combination of red and green fluorescence. *White line*, The boundary between the Rathke's pouch and the developing anterior lobe. A, Anterior lobe; RP, Rathke's pouch; P, posterior lobe. The number of mice analyzed was *Prop1*$^{+/+}$, n =4; *Prop1*$^{df/df}$, n =4; *Prop1*$^{null/null}$, n =1.

proliferative zone to the anterior lobe. Whether the change in localization is passive or active remains to be determined. These experiments were replicated with the *Prop1*$^{df/df}$ mice, at the N4 generation of backcross to C57BL/6J (data not shown), and on the noninbred DF/B stock (Fig. 4, G–I). At e14.5, the dwarf pituitary is well populated with cells labeled at e11.5 with IdU (Fig. 4, G and I), and the majority of cells labeled at e12.5 with BrdU are retained in the perilumenal zone of the *Prop1*$^{df/df}$ pituitaries (Fig. 4, H and I), suggesting that the migration of these cells from the proliferative zone to the anterior lobe is impaired. This migration defect is more evident in the *Prop1*$^{null/null}$ pituitary. Cells labeled at e11.5 migrate into the anterior lobe (Fig. 4, J and L); however, very few cells labeled at e12.5 are seen in the anterior lobe at e14.5 (Fig. 4, K and L). The difference between the *Prop1*$^{df/df}$ and the *Prop1*$^{null/null}$ mice may indicate that the block in migration is less complete in df/df mutants, or it may reflect another influence of genetic background, as the null/null mice examined were on a mixed background of 129 substrains. Nevertheless, in all mutants, and regardless of background, cells proliferating at e12.5 predominated in the perilumenal area instead of colonizing the anterior lobe.

To determine the identity of the mislocalized cells in the *Prop1*$^{df/df}$ pituitary, MSH and proopiomelanocortin (POMC) expression were examined in wild-type and Ames dwarf pituitaries on the day of birth (P1). POMC is cleaved via proteolysis to produce ACTH in the anterior lobe (45, 46) and MSH in the intermediate lobe of the pituitary gland (47). POMC is expressed in the intermediate lobe as well as throughout the anterior lobe of the wild-type pituitary gland (Fig. 5A) and the *Prop1*$^{df/df}$ pituitary gland (Fig. 5B). MSH is expressed only in the intermediate lobe of the wild-type gland (Fig. 5C). In the Ames dwarf, MSH is only expressed in the collapsed pouch regions that make contact with the posterior lobe (Fig. 5D), which suggests that most of the mislocalized cells have not differentiated as intermediate lobe hormone-secreting cells.

Increased Apoptosis in Ames Dwarf Pituitaries after Birth

After birth there are fewer proliferating cells in *Prop1*$^{df/df}$ pituitaries compared with wild-type mice, and the mutant organ fails to increase in volume after P8. To determine whether mutant pituitaries exhibit increased apoptosis in addition to the reduced proliferation, we examined the number of dying cells in both the wild-type and dwarf pituitaries at P1 and P8 using the terminal deoxynucieotidyl transferase-mediated deoxyuridine triphosphate nick end labeling (TUNEL) assay, which labels the ends of nicked DNA (48). At P1 (data not shown) and P8, there are obviously more apoptotic cells in dwarf pituitaries than wild type (compare Fig. 5E, E′, *arrowheads*; and 5F, F′, *arrowheads*). To quantify the extent of the increase in apoptosis, cell counts were carried out on serial sections in wild-type and dwarf pituitaries at these times. At birth (P1), dwarf pituitaries had approximately 3-fold more cell death than wild type, 47 apoptotic cells per pituitary slice $\pm$ 12 *vs.* 15 $\pm$ 4, (Fig. 5G, *left*). The apoptotic cell counts at P8 were normalized for pituitary area to take into account the smaller size of the *Prop1*^{df} organ at this time. Approximately 3-fold more apoptotic cells were observed per 50,000 μm^2 of *Prop1*^{dfdf} pituitary cells compared with the wild type, 17 $\pm$ 5 *vs.* 6 $\pm$ 1, (Fig. 5G, *right*). Thus, the 3-fold enhancement in apoptosis in *Prop1*$^{df/df}$ pituitaries relative to wild type is consistent at P1 and P8. The decrease in proliferation and increase in cell death accounts for the lack of growth of Ames dwarf pituitaries after birth and suggests that cells that are unable to differentiate are destined to die, resulting in degeneration of the mutant pituitary gland.

DISCUSSION

Mutations in the transcription factor PROP1 cause pituitary hormone deficiency in mice and humans. *Prop1*$^{df/df}$ mice have profound pituitary hypoplasia as adults, and the pituitary primordium of *Prop1*$^{df/df}$ mutants is dysmorphic with slightly smaller prospective anterior lobe and apparently overgrown Rathke's pouch at e14.5 (20, 22, 36). The mechanism whereby *Prop1* deficiency causes this dysmorphology and hypoplasia had been elusive, as no difference in proliferation or cell death is evident at e12.5 or e14.5 (36). Our studies suggest that the role of *Prop1* in development and growth of the pituitary is to promote the release of progenitor cells from Rathke's pouch into the anterior lobe. In the absence of functional *Prop1,* pituitary progenitor cells fail to express *Notch2* (26), prematurely cease expression of *cyclin D2*, and are abnormally retained within the perilumenal area of the pouch, causing the pouch to take on an overgrown, dysmorphic appearance. The overall size of the developing organ is not profoundly hypoplastic until the mice are 1–2 wk old, long after *Prop1* expression has normally waned. The hypoplasia involves both programmed cell death and reduced proliferation after birth. These studies demonstrate the importance of *Prop1* in early pituitary development and define the legacy of *Prop1* deficiency on future organ growth. These observations suggest that the pituitary hyperplasia in humans deficient in *PROP1* could be due to trapped progenitor cells and the subsequent degeneration could be due to apoptosis of undifferentiated cells.

During early pituitary organogenesis (e10.5–14.5), cells proliferating at the highest rate are localized at the dorsal aspect of Rathke's pouch, nearest the infundibulum (35). The infundibulum produces factors that induce differentiation in Rathke's pouch, including members of the bone morphogenetic protein, FGF, and WNT gene families (30–32). Thus, it makes sense that the highest rate of proliferation is within the part of

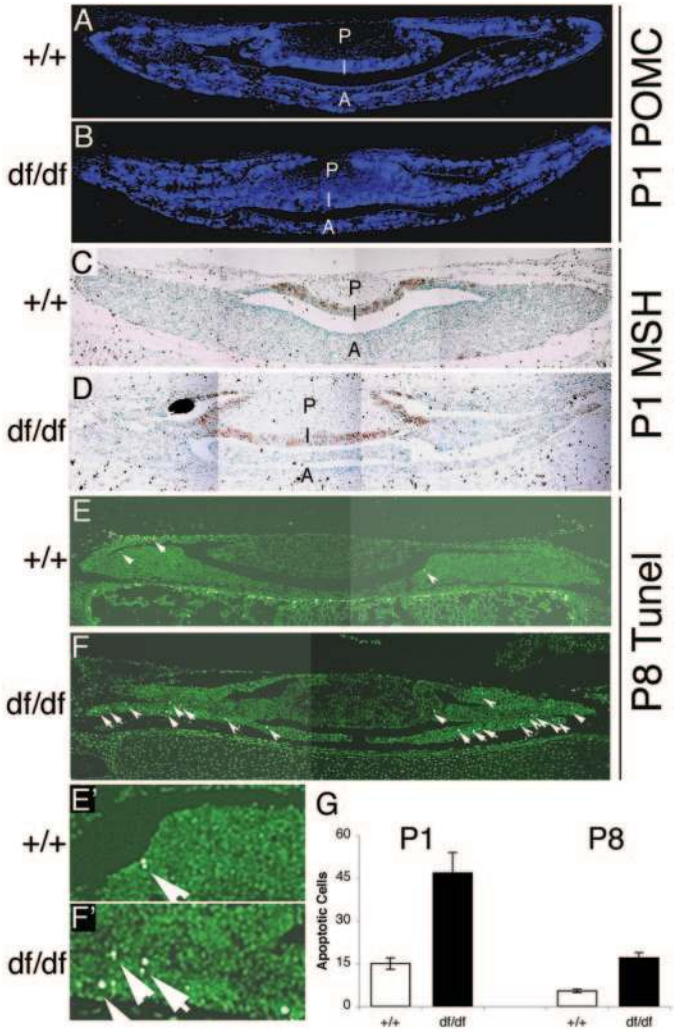

Fig. 5. MSH Expression and Apoptosis in Wild-Type and *Prop1*$^{df/df}$ P1 Pituitaries

POMC (*blue*) expression is detected in the intermediate lobe and anterior lobe of both wild-type (A) and dwarf (B) P1 pituitaries. α-MSH (*brown*) expression is detected only in the intermediate lobe of P1 wild-type pituitaries (C). MSH is detected in the regions of the tissue that contact the posterior lobe in the Ames dwarf pituitary (D). Methyl *green* counterstain was used with the MSH immunhistochemistry (C and D). P, Posterior lobe; I, intermediate lobe; A, anterior lobe. Original magnification, $\times$200. TUNEL staining of P8 pituitaries (*bright white cells*) reveals an increase in apoptotic cells in *Prop1*$^{df/df}$ (F and F′, *arrowheads*) compared with wild type (E and E′, *arrowheads*). G, The average number of apoptotic cells at P1 (*left*) and P8 (*right*) is significantly increased in *Prop1*$^{df/df}$ pituitaries (*black bars*) compared with wild-type pituitaries (*white bars*) at both ages. P8 apoptotic cell counts were normalized for pituitary area (apoptotic cells per 5×10^4 μm^2). The number of animals analyzed at each time point and statistical significance is as follows (n = +/+ and df/df): P1, n = 3 and 3, $P < 0.01$; P8, n = 6 and 8; $P < 0.001$.

the pouch that is closest to these growth factors. Apparently *Prop1*-deficient pituitaries initially respond to the secreted factors that stimulate proliferation because the total cellular volume of the pituitary increases approximately 20-fold from e12.5 to birth in both mutant and normal pituitaries.

The cells around the lumen of Rathke's pouch are organized as a tightly packed columnar layer during gestation, whereas the cells within the anterior lobe are more loosely packed, giving the tissue a glandular appearance. We show that cells originating in the pouch normally colonize the anterior lobe, concomitant with cessation of DNA synthesis and silencing of *cyclin D2* and *Notch2* gene expression. In *Prop1*-deficient mice, some cells leave the pouch and initiate formation of the anterior lobe, but the majority are retained within the pouch, retaining dense packing and causing the characteristic organ dysmorphology. The failure of *Prop1*-deficient mice to initiate *Notch2* expression at this time may contribute to the retention of anterior lobe progenitors in the pouch (26). This idea is supported by the role that Notch signaling plays in regulation of precursor cell differentiation in nervous system development (49–51). In contrast to normal mice, *Prop1*-deficient cells leave the cell cycle while they are still in the perilumenal area, and they are

severely compromised in detachment and movement to the anterior lobe. The movement might normally involve changes in cell adhesion, resulting in release of cells, followed by either active migration toward factors produced in the ventral mesenchyme or passive movement away from the pouch as more cells detach and fill in the available space between the brain and sphenoid cartilage. There are numerous examples of cell adhesion molecules and components of the extracellular matrix playing roles in cell migration during organogenesis, including mouse thyroid (52), liver (53), lung (54), and kidney (55) development. We observed no obvious changes in expression of E-cadherin (data not shown), but there are many other cell adhesion molecules and extracellular matrix components expressed in normal pituitary glands that could be involved (56).

The mouse pituitary gland normally continues to grow in late gestation and early neonatal life, expanding in size approximately 14-fold from birth to adulthood. We report here that proliferating cells are scattered throughout the anterior lobe of normal newborn and adult mice, instead of being concentrated in the perilumenal area of Rathke's pouch. *Prop1*-deficient mice, however, have very few proliferating cells in the anterior lobe at the same age. The mutant pituitaries grow very little from birth to P15, when the cells within the dysmorphic pouch die.

Various BrdU labeling studies in rats have suggested that a significant fraction of differentiated pituitary cells are proliferating during late embryonic development and early postnatal life. For example, approximately 7% and approximately 3.5% of corticotropes appear to be replicating during late fetal development and early postnatal life, respectively (57). In addition, the thyrotrope population increases significantly after birth, when it was estimated that approximately 20% of thyrotropes were derived from preexisting thryotropes. Also, a quarter of somatotropes were proliferating at 3 wk of age (58, 59). Transgene ablation experiments in mice suggest that, although the majority of gonadotropes are postmitotic, somatotropes are actively dividing and have the ability to regenerate (60–62). Although the identity of pituitary precursors or stem cells is not known, folliculostellate cells, a nonendocrine, supporting cell type in the pituitary, can differentiate into skeletal muscle, suggesting that these multipotent cells could be pituitary precursors (63–65). Regardless of the nature of the precursor cells within the developing anterior lobe, normal pituitaries have the capacity to grow and regenerate, whereas *Prop1*-deficient pituitaries exhibit differentiation failure, which may account for the increase in apoptosis after birth and subsequent failure of the organ to grow beyond d 8–11 of postnatal life.

Very few apoptotic cells are detectable during normal pituitary organogenesis, in contrast to some developmental processes that involve extensive tissue remodeling and cell death (66). Cell death is enhanced in the pituitary in certain pathological conditions, such as failure in FGF signaling (31, 67, 68) and deficiency of some transcription factors, including LHX4 and PITX2 (Ref. 36; and Charles, M. A., H. Suh, T. A. Hjalt, J. Drouin, S. A. Camper, and P. J. Gage, unpublished). We report here that *Prop1* deficiency also leads to cell death, although the onset of apoptosis is much later in *Prop1* mutants than in the previous examples. Apoptosis occurs in *Prop1* mutants long after signaling from the infundibulum has taken place. This suggests that a different trigger is responsible for apoptosis in *Prop1*-deficient mice, such as the inability precursor cells to differentiate. There are precedents for this from a number of systems. For example, primordial germ cells that fail to migrate to the genital ridges undergo apoptosis, and both PC12 cells and human epidermal keratinocytes are more sensitive to apoptosis before differentiation (69–71).

This study provides a clue as to the mechanism whereby *PROP1* deficiency causes pituitary dysmorphology and hypoplasia (Fig. 6). Proliferating cells, either precursors or pituitary stem cells, normally migrate into the expanding anterior lobe from the ventral portion of the Rathke's pouch early in pituitary development. The pituitaries of young *PROP1*-deficient patients usually appear to be hyperplastic by magnetic resonance imaging, and the overgrowth usually resolves before adulthood, resulting in a hypoplastic organ. We propose that the pituitary overgrowth in human patients is analogous to the undifferentiated cells trapped in the perilumenal area of *Prop1*-deficient mice, and the resolution is due to degeneration of undifferentiated cells by apoptosis. This is consistent with the suggestion that the hyperplasia is due to mislocalized cells and anecdotal evidence that the hyperplastic pituitaries contain undifferentiated cells (37, 72). We also propose that the gradual loss of hormones in *PROP1*-deficient patients is due to the depletion of precursor pools. The loss of hormones is not as severe in mice as it is in humans. This disparity has been observed in other mouse models, such as the dystrophin-deficient mice, which only develop signs of muscular weakness very late in life compared with the severe muscular dystrophy characteristic of young human patients, probably because they have a higher capacity for muscle regeneration in relation to their life span (39, 73).

In summary, we have demonstrated a role for PROP1 in progenitor migration from Rathke's pouch into the developing anterior lobe. The overall growth of the mutant pituitary is reduced in older animals due to the developmental defect. These studies provide valuable insight into the mechanism of PROP1 action in pituitary development and disease.

MATERIALS AND METHODS

Mice

Ames dwarf mice (DF/B-*df*/*df*) were originally obtained from Dr. A. Bartke (Southern Illinois University, Carbondale, IL) and have been maintained in our colony. Ames *Prop1*$^{+/df}$ het-

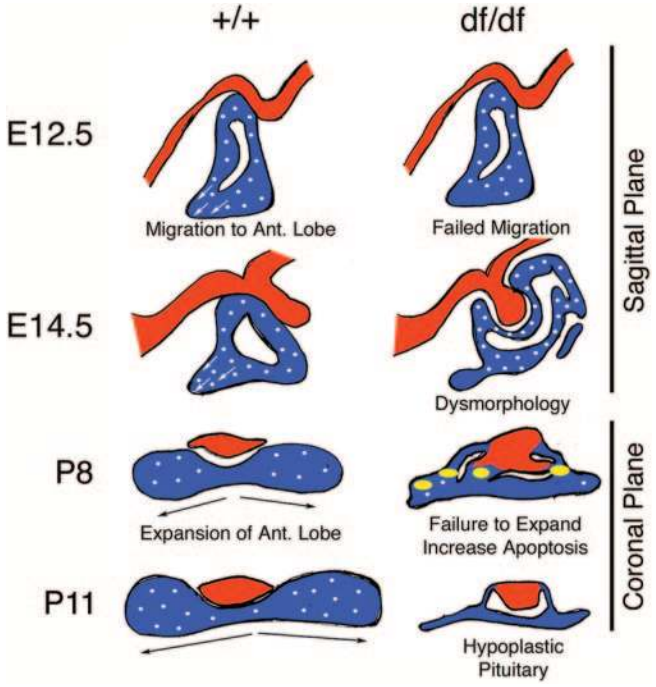

Fig. 6. Model of Pituitary Growth in Normal and *Prop1*-Deficient Mice

During gestation (e12.5, e14.5), cells surrounding the lumen of Rathke's pouch (*blue*) receive growth-promoting signals from the developing posterior lobe (neural ectoderm, *red*) and are released from the proliferative zone to populate the anterior lobe (*white dots*). The anterior lobe normally expands laterally after birth (P8, P11), and this growth is driven by actively proliferating cells within the anterior lobe. From the peak time of normal *Prop1* expression (e12.5 onward), *Prop1*-deficient mice have a deficit of cells in the anterior lobe because they are not released from the proliferative region. Continued growth without release of the cells results in the appearance of an overgrown, dysmorphic Rathke's pouch and hypoplastic anterior lobe. By P8 the cells that did not differentiate undergo apoptosis (*yellow ovals*). Little or no proliferating cells are detectable in the hypoplastic anterior pituitary of *Prop1*-deficient mice at P11 because the progenitors did not colonize the anterior lobe.

erozygous mice were repeatedly back-crossed onto the C57BL/6J background (The Jackson Laboratories, Bar Harbor, ME) to generate the N7 C57BL/6J $Prop1^{df}$ mice. $Prop1^{null}$ mice were generated in R1 ES cells and back-crossed to C57BL/6J (N4) and the 129S1/SvImJ (N2) (The Jackson Laboratories) background (21). $Prop1^{df}$ and wild-type mice on the Ames DF/B background were used for the H&E, BrdU, volumetrics, and apoptosis studies. The $Prop1^{df}$ DF/B, $Prop1^{df}$ C57BL/6J, $Prop1^{null}$ C57BL/6J, and $Prop1^{null}$ 129S1/SvImJ mice were used for the BrdU/IdU pulse-chase studies. The morning after conception is designated e0.5, and the day of birth is designated as P1. All mice were housed in a 12-h light, 12-h dark cycle with unlimited access to tap water and Purina 5008 or 5020 chows. All procedures using mice were approved by the University of Michigan Committee on Use and Care of Animals, and all experiments were conducted in accordance with the principles and procedures outlined in the NIH Guidelines for the Care and Use of Experimental Animals.

PCR Genotyping

The genotype of $Prop1^{df}$ mice was determined by PCR amplification with the forward primer 5′-GAGCTGGGGAGAC-CTAAGCTTTGCC- 3′ and reverse primer 5′-GCCCAGATGT-CAGGATACTG-3′ to produce a 135-bp band. Restriction digestion with *Hin*fI generates 97- and 40-bp bands specific to the wild-type allele, whereas the $Prop1^{df}$ mutant allele is uncut. The genotype of $Prop1^{null}$ mice was determined by PCR amplification with the forward primer 5′-GTGAGAAAA-CAGGTATCTAGCT-3′ (specific for both the wild-type and targeted allele); reverse primer 1, 5′-TTCGTTTGCTTTTCCT-GATG-3′ (specific to the wild-type allele); and reverse primer 2, 5′-CCACTTTGCGTTTCTTCTTGG-3′ (specific to LacZ in targeted allele) to generate the 240-bp band for the targeted allele and a 270-bp band for the wild-type allele.

Histology and Immunohistochemistry

$Prop1^{+/+}$, $Prop1^{+/df}$, and $Prop1^{df/df}$ ($Prop1^{df}$) embryos or litters were generated from mating $Prop1^{+/df}$ heterozygotes. $Prop1^{+/+}$, $Prop1^{+/-}$, and $Prop1^{-/-}$ ($Prop1^{null}$) embryos were generated from mating $Prop1^{+/-}$ heterozygotes. Embryos and mouse heads were fixed for 2–24 h in 4% paraformaldehyde in PBS (PBS, pH 7.2). All samples were washed in PBS, dehydrated in a graded series of ethanol, and embedded in paraffin. Six-micrometer sections were prepared and either stained with H&E or processed as described below.

To detect cell proliferation in fetuses, pregnant mice were injected ip with BrdU at 100 mg/g body weight, 2 h before embryo retrieval (43). To examine proliferation in the pituitary during postnatal development, individual mouse pups were injected ip with BrdU at 100 mg/g body weight and killed 2 h later. After epitope retrieval in 2 N HCl, BrdU incorporation was examined with a rat anti-BrdU antibody (1:200; Harlan Sera, Belton, UK) and detected with a FITC-labeled secondary antibody (1:200; Jackson ImmunoResearch Laboratories, West Grove, PA). In some cases, sections were counterstained with the nuclear counterstain 7-aminoactinomycin D (Molecular Probes, Eugene, OR).

For the IdU/BrdU pulse-chase experiment, pregnant mice were injected ip with IdU at e11.5 at 100 mg/g body weight

and then injected ip with BrdU at e12.5 at 100 mg/g body weight. Embryos were harvested at e14.5. After antigen retrieval with 10 mM citrate boiling for 10 min, BrdU was detected with a rat anti-BrdU antibody (1:200; Harlan) and a biotin-conjugated antirat IgG antibody (1:400; Jackson Immunoresearch) using the tyramide signal amplification (TSA) Fluoresceine (FITC) kit (according to the manufacturer's protocol; PerkinElmer, Boston, MA). IdU was detected with a mouse anti-IdU/BrdU antibody (1:200; Caltag, Burlingame, CA) and a biotin-conjugated antimouse IgG antibody (1:400; Jackson ImmunoResearch Laboratories) using the TSA TRITC kit (PerkinElmer). To distinguish pituitary cells from the surrounding mesenchyme, PITX1 was detected with a rabbit anti-PITX1 antibody (1:1500; J. Drouin, Institut de Recherches Cliniques de Montreal, Montreal, Quebec, Canada) and a biotin-conjugated antirabbit IgG antibody (1:400; Jackson ImmunoResearch Laboratories) using the TSA coumarin kit (PerkinElmer). The sections were incubated sequentially with the PITX1, BrdU, and IdU/BrdU antibodies overnight, and a biotin/avidin blocking kit (Vector Laboratories, Burlingame, CA) was used to prevent cross-reactivity. Sections were incubated with 0.1% Sudan Black B (Fisher Scientific, Fair Lawn, NJ) in 70% ethanol for 30 min before coverslip mounting to prevent autofluorescence of red blood cells. Cells that were labeled with BrdU were detected by both the IdU/BrdU and BrdU antibodies and appear yellow as a result of the combination of FITC and TRITC fluorophores.

Programmed cell death in the pituitaries was detected by the TUNEL method using either the FragEL kit (according to the manufacturer's protocol; Oncogene Research Products, La Jolla, CA) or the *in situ* cell detection kit POD (Roche, Indianapolis, IN). Sections were counterstained with the nuclear counterstain 4,6-diamidino-2-phenylindole, dihydrochloride (DAPI; Molecular Probes). Apoptotic cells were counted on four to eight pituitary slices per animal and three to eight animals per genotype. Apoptotic cell counts were averaged for wild type and *Prop1*^{df} at each age. P8 apoptotic cell counts were normalized for area (per 50,000 μm^2) by capturing digital images of the DAPI-counterstained sections with a Leitz DMRB microscope (W. Nuhsbaum, Inc., McHenry, IL) and an Optronics (Goleta, CA) camera and processed with SURFdriver 3.5 Software (Kailua, HI) for the area estimates. Student's *t* test was used to determine statistical significance.

Cyclin D2 was examined with a rabbit anti-cyclin D2 antibody (1:500; Santa Cruz Biotechnology, Santa Cruz, CA) after antigen retrieval with 10 mM citrate boiling and detected with a biotin-conjugated antirabbit IgG (1:400; Vector Laboratories) followed by a streptavidin-conjugated Cy3 fluorophore (1:200; Jackson ImmunoResearch). Ki67 was examined with a rabbit polyclonal anti-Ki67 antibody (1:500; NovoCastra, Newcastle, UK) after antigen retrieval with 10 mM citrate boiling and detected with a biotin-conjugated antirabbit IgG followed by a streptavidin-conjugated Cy2 fluorophore (1:200; Jackson ImmunoResearch Laboratories).

POMC was examined with a rabbit antihuman ACTH antibody (1:1800; National Institute of Diabetes and Digestive Kidney Diseases, Torrance, CA) and detected with a biotin-conjugated antirabbit IgG using the TSH coumarin kit (PerkinElmer). MSH was examined with a sheep anti-MSH antibody (1:10,000; Chemicon, Temecula, CA) and detected with a biotin-conjucted antisheep IgG (1:500; Jackson ImmunoResearch Laboratories) using the Vectastain ABC kit (according to manufacturer's protocol; Vector Laboratories).

Volumetrics

Volumetrics and three-dimensional modeling was performed by staining serial sections with H&E. Digital images of these pituitary sections were captured with a Leitz DMRB microscope and an Optronics camera and processed with the SURFdriver software for three-dimensional reconstruction and volume estimation. Three to five animals were used for each genotype at each age. Student's *t* test was used to determine statistical significance. ANOVA was used to determine statistical significance across multiple ages.

Acknowledgments

We thank Jacques Drouin for the generous gift of the PITX1 antibody and Mohamed H. Farah, Tom Glaser, Deb Gumucio, Gary Hammer, and Phil Gage for their suggestions.

Received September 1, 2004. Accepted November 29, 2004.

Address all correspondence and requests for reprints to: Sally A. Camper, 4301 Medical Science Research Building III, 1500 West Medical Center Drive, Ann Arbor, Michigan 48109-0638. E-mail: scamper@umich.edu.

This work was funded by the National Institutes of Health (Grants T32 GM07863 and T32 GM07315 to R.D.W., Grant NRSA F32 DK60306 to L.T.R., Grant T32 GM07315 to I.O.N., and Grants R37 HD30428 and R01 HD34283 to S.A.C.), the University of Michigan Rackham Graduate School (H.S.) and Undergraduate Research Opportunity Program (B.M.S.), and The Endocrine Society (B.M.S.).

Current address for H.S.: Salk Institute for Biological Studies, P.O. Box 85800, San Diego, California 92186-5800. E-mail: suh@salk.edu.

Current address for I.O.N.: Department of Pathology/Neuropathology, Johns Hopkins University, Ross Research Building, Baltimore, Maryland 21205. E-mail: igor.nasonkin@jhmi.edu.

REFERENCES

1. Procter AM, Phillips 3rd JA, Cooper DN 1998 The molecular genetics of growth hormone deficiency. Hum Genet 103:255–272
2. Vimpani GV, Vimpani AF, Lidgard GP, Cameron EHD, Farquhar JW 1977 Prevalence of severe growth hormone deficiency. BMJ 2:427–430
3. Braga S, Phillips JA, 3rd, Joss E, Schwarz H, Zuppinger K 1986 Familial growth hormone deficiency resulting from a 7.6 kb deletion within the growth hormone gene cluster. Am J Med Genet 25:443–452
4. Mullis P, Patel M, Brickell PM, Brook CG 1990 Isolated growth hormone deficiency: analysis of the growth hormone (GH)-releasing hormone gene and the GH gene cluster. J Clin Endocrinol Metab 70:187–191
5. Cogan JD, Wu W, Phillips 3rd JA, Arnhold IJ, Agapito A, Fofanova OV, Osorio MG, Bircan I, Moreno A, Mendonca BB 1998 The PROP1 2-base pair deletion is a common cause of combined pituitary hormone deficiency. J Clin Endocrinol Metab 83:3346–3349
6. Mendonca BB, Osorio MG, Latronico AC, Estefan V, Lo LS, Arnhold IJ 1999 Longitudinal hormonal and pituitary imaging changes in two females with combined pituitary hormone deficiency due to deletion of A301,G302 in the PROP1 gene. J Clin Endocrinol Metab 84:942–945
7. Wu W, Cogan JD, Pfaffle RW, Dasen JS, Frisch H, O'Connell SM, Flynn SE, Brown MR, Mullis PE, Parks JS, Phillips 3rd JA, Rosenfeld MG 1998 Mutations in PROP1 cause familial combined pituitary hormone deficiency. Nat Genet 18:147–149
8. Pfaffle RW, DiMattia GE, Parks JS, Brown MR, Wit JM, Jansen M, Van der Nat H, Van den Brande JL, Rosenfeld MG, Ingraham HA 1992 Mutation of the POU-specific domain of Pit-1 and hypopituitarism without pituitary hypoplasia. Science 257:1118–1121

9. Radovick S, Nations M, Du Y, Berg LA, Weintraub BD, Wondisford FE 1992 A mutation in the POU-Homeodomain of Pit-1 responsible for combined pituitary hormone deficiency. Science 257:1115–1117
10. Tajima T, Hattorri T, Nakajima T, Okuhara K, Sato K, Abe S, Nakae J, Fujieda K 2003 Sporadic heterozygous frameshift mutation of HESX1 causing pituitary and optic nerve hypoplasia and combined pituitary hormone deficiency in a Japanese patient. J Clin Endocrinol Metab 88:45–50
11. Netchine I, Sobrier ML, Krude H, Schnabel D, Maghnie M, Marcos E, Duriez B, Cacheux V, Moers A, Goossens M, Gruters A, Amselem S 2000 Mutations in LHX3 result in a new syndrome revealed by combined pituitary hormone deficiency. Nat Genet 25:182–186
12. Machinis K, Pantel J, Netchine I, Leger J, Camand OJ, Sobrier ML, Dastot-Le Moal F, Duquesnoy P, Abitbol M, Czernichow P, Amselem S 2001 Syndromic short stature in patients with a germline mutation in the LIM homeobox LHX4. Am J Hum Genet 69:961–968
13. Cohen LE, Wondisford FE, Radovick S 1996 Role of Pit-1 in the gene expression of growth hormone, prolactin, and thyrotropin. Endocrinol Metab Clin North Am 25:523–540
14. Deladoey J, Fluck C, Buyukgebiz A, Kuhlmann BV, Eble A, Hindmarsh PC, Wu W, Mullis PE 1999 "Hot spot" in the PROP1 gene responsible for combined pituitary hormone deficiency. J Clin Endocrinol Metab 84:1645–1650
15. Agarwal G, Bhatia V, Cook S, Thomas PQ 2000 Adrenocorticotropin deficiency in combined pituitary hormone deficiency patients homozygous for a novel PROP1 deletion. J Clin Endocrinol Metab 85:4556–4561
16. Vallette-Kasic S, Barlier A, Manavela M, Teinturier C, Brue T, Two hot spots in the PROP1 gene of patients with multiple pituitary hormone deficiency. Program of the 82nd Annual Meeting of The Endocrine Society, Toronto, Canada, 2000, p 448 (Abstract 1851)
17. Fluck C, Deladoey J, Rutishauser K, Eble A, Marti U, Wu W, Mullis PE 1998 Phenotypic variability in familial combined pituitary hormone deficiency caused by a *PROP1* gene mutation resulting in the substitution of Arg→Cys at codon 120 (R120C). J Clin Endocrinol Metab 83: 3727–3734
18. Bottner A, Keller E, Kratzsch J, Stobbe H, Weigel JF, Keller A, Hirsch W, Kiess W, Blum WF, Pfaffle RW 2004 PROP1 mutations cause progressive deterioration of anterior pituitary function including adrenal insufficiency: a longitudinal analysis. J Clin Endocrinol Metab 89: 5256–5265
19. Riepe FG, Partsch CJ, Blankenstein O, Monig H, Pfaffle RW, Sippell WG 2001 Longitudinal imaging reveals pituitary enlargement preceding hypoplasia in two brothers with combined pituitary hormone deficiency attributable to PROP1 mutation. J Clin Endocrinol Metab 86: 4353–4357
20. Sornson MW, Wu W, Dasen JS, Flynn SE, Norman DJ, O'Connell SM, Gukovsky I, Carriere C, Ryan AK, Miller AP, Zuo L, Gleiberman AS, Andersen B, Beamer WG, Rosenfeld MG 1996 Pituitary lineage determination by the *Prophet* of *Pit-1* homeodomain factor defective in Ames dwarfism. Nature 384:327–333
21. Nasonkin IO, Ward RD, Raetzman LT, Seasholtz AF, Saunders TL, Gillespie PJ, Camper SA 2004 Pituitary hypoplasia and respiratory distress syndrome in *Prop1* knockout mice. Hum Mol Genet 13:2727–2735
22. Gage PJ, Brinkmeier ML, Scarlett LM, Knapp LT, Camper SA, Mahon KA 1996 The Ames dwarf gene, df, is required early in pituitary ontogeny for the extinction of *Rpx* transcription and initiation of lineage specific cell proliferation. Molecular Endocrinology 10:1570–1581
23. Camper SA, Saunders TL, Katz RW, Reeves RH 1990 The *Pit-1* transcription factor gene is a candidate for the Snell dwarf mutation. Genomics 8:586–590
24. Li S, Crenshaw 3rd EB, Rawson EJ, Simmons DM, Swanson LW, Rosenfeld MG 1990 Dwarf locus mutants lacking three pituitary cell types result from mutations in the POU-domain gene *Pit-1*. Nature 347:528–533
25. Tang K, Bartke A, Gardiner CS, Wagner TE, Yun JS 1993 Gonadotropin secretion, synthesis, and gene expression in human growth hormone transgenic mice and in Ames dwarf mice. Endocrinology 132:2518–2524
26. Raetzman LT, Ross SA, Cook S, Dunwoodie SL, Camper SA, Thomas PQ 2004 Developmental regulation of Notch signaling genes in the embryonic pituitary: *Prop1* deficiency affects *Notch2* expression. Dev Biol 265:329–340
27. Buckwalter MS, Katz RW, Camper SA 1991 Localization of the panhypopituitary dwarf mutation (*df*) on mouse chromosome 11 in an intersubspecific backcross. Genomics 10:515–526
28. Burrows HL, Douglas KR, Seasholtz AF, Camper SA 1999 Genealogy of the anterior pituitary gland: tracing a family tree. Trends Endocrinol Metab 10:343–352
29. Watkins-Chow DE, Camper SA 1998 How many homeobox genes does it take to make a pituitary gland? Trends Genet 14:284–290
30. Ericson J, Norlin S, Jessell TM, Edlund T 1998 Integrated FGF and BMP signaling controls the progression of progenitor cell differentiation and the emergence of pattern in the embryonic anterior pituitary. Development 125: 1005–1015
31. Takuma N, Sheng HZ, Furuta Y, Ward JM, Sharma K, Hogan BL, Pfaff SL, Westphal H, Kimura S, Mahon KA 1998 Formation of Rathke's pouch requires dual induction from the diencephalon. Development 125: 4835–4840
32. Treier M, Gleiberman AS, O'Connell SM, Szeto DP, McMahon JA, McMahon AP, Rosenfeld MG 1998 Multistep signaling requirements for pituitary organogenesis in vivo. Genes Dev 12:1691–1704
33. Yamaguchi TP, Bradley A, McMahon AP, Jones S 1999 A Wnt5a pathway underlies outgrowth of multiple structures in the vertebrate embryo. Development 126: 1211–1223
34. Rizzoti K, Brunelli S, Carmignac D, Thomas PQ, Robinson IC, Lovell-Badge R 2004 SOX3 is required during the formation of the hypothalamo-pituitary axis. Nat Genet 36:247–255
35. Ikeda H, Yoshimoto T 1991 Developmental changes in proliferative activity of cells of the murine Rathke's pouch. Cell Tissue Res 263:41–47
36. Raetzman LT, Ward R, Camper SA 2002 *Lhx4* and *Prop1* are required for cell survival and expansion of the pituitary primordia. Development 129:4229–4239
37. Voutetakis A, Argyropoulou M, Sertedaki A, Livadas S, Xekouki P, Maniati-Christidi M, Bossis I, Thalassinos N, Patronas N, Dacou-Voutetakis C 2004 Pituitary magnetic resonance imaging in 15 patients with Prop1 gene mutations: pituitary enlargement may originate from the intermediate lobe. J Clin Endocrinol Metab 89: 2200–2206
38. Cheng TC, Beamer WG, Phillips 3rd JA, Bartke A, Mallonee RL, Dowling C 1983 Etiology of growth hormone deficiency in Little, Ames, and Snell dwarf mice. Endocrinology 113:1669–1678
39. Pastoret C, Sebille A 1995 mdx Mice show progressive weakness and muscle deterioration with age. J Neurol Sci 129:97–105
40. Reed SI 1997 Control of the G1/S transition. Cancer Surv 29:7–23
41. Gerdes J, Lemke H, Baisch H, Wacker HH, Schwab U, Stein H 1984 Cell cycle analysis of a cell proliferation-associated human nuclear antigen defined by the monoclonal antibody Ki-67. J Immunol 133:1710–1715
42. Packard Jr DS, Menzies RA, Skalko RG 1973 Incorportaiton of thymidine and its analogue, bromodeoxyuridine,

into embryos and maternal tissues of the mouse. Differentiation 1:397–404
43. Nowakowski RS, Lewin SB, Miller MW 1989 Bromodeoxyuridine immunohistochemical determination of the lengths of the cell cycle and the DNA-synthetic phase for an anatomically defined population. J Neurocytol 18: 311–318
44. Julian D, Ennis K, Korenbrot JI 1998 Birth and fate of proliferative cells in the inner nuclear layer of the mature fish retina. J Comp Neurol 394:271–282
45. Japon MA, Rubinstein M, Low MJ 1994 In situ hybridization analysis of anterior pituitary hormone gene expression during fetal mouse development. J Histochem Cytochem 42:1117–1125
46. Elkabes S, Loh YP, Nieburgs A, Wray S 1989 Prenatal ontogenesis of pro-opiomelanocortin in the mouse central nervous system and pituitary gland: an in situ hybridization and immunocytochemical study. Brain Res Dev Brain Res 46:85–95
47. Civelli O, Birnberg N, Herbert E 1982 Detection and quantitation of pro-opiomelanocortin mRNA in pituitary and brain tissues from different species. J Biol Chem 257:6783–6787
48. Gavrieli Y, Sherman Y, Ben-Sasson SA 1992 Identification of programmed cell death in situ via specific labeling of nuclear DNA fragmentation. J Cell Biol 119:493–501
49. Beatus P, Lendahl U 1998 Notch and neurogenesis. J Neurosci Res 54:125–136
50. Lewis J 1998 Notch signalling and the control of cell fate choices in vertebrates. Semin Cell Dev Biol 9:583–589
51. Gaiano N, Fishell G 2002 The role of notch in promoting glial and neural stem cell fates. Annu Rev Neurosci 25: 471–490
52. Fagman H, Grande M, Edsbagge J, Semb H, Nilsson M 2003 Expression of classical cadherins in thyroid development: maintenance of an epithelial phenotype throughout organogenesis. Endocrinology 144:3618–3624
53. Zaret KS 2002 Regulatory phases of early liver development: paradigms of organogenesis. Nat Rev Genet 3:499–512
54. Warburton D, Schwarz M, Tefft D, Flores-Delgado G, Anderson KD, Cardoso WV 2000 The molecular basis of lung morphogenesis. Mech Dev 92:55–81
55. Dahl U, Sjodin A, Larue L, Radice GL, Cajander S, Takeichi M, Kemler R, Semb H 2002 Genetic dissection of cadherin function during nephrogenesis. Mol Cell Biol 22:1474–1487
56. Carninci P, Waki K, Shiraki T, Konno H, Shibata K, Itoh M, Aizawa K, Arakawa T, Ishii Y, Sasaki D, Bono H, Kondo S, Sugahara Y, Saito R, Osato N, Fukuda S, Sato K, Watahiki A, Hirozane-Kishikawa T, Nakamura M, Shibata Y, Yasunishi A, Kikuchi N, Yoshiki A, Kusakabe M, *et al.* 2003 Targeting a complex transcriptome: the construction of the mouse full-length cDNA encyclopedia. Genome Res 13:1273–1289
57. Taniguchi Y, Kominami R, Yasutaka S, Kawarai Y 2000 Proliferation and differentiation of pituitary corticotrophs during the fetal and postnatal period: a quantitative immunocytochemical study. Anat Embryol (Berl) 201: 229–234
58. Taniguchi Y, Yasutaka S, Kominami R, Shinohara H 2001 Proliferation and differentiation of thyrotrophs in the pars distalis of the rat pituitary gland during the fetal and postnatal period. Anat Embryol (Berl) 203:249–253
59. Carbajo-Perez E, Motegi M, Watanabe YG 1989 Cell proliferation in the anterior pituitary of mice during growth. Biomedical Research 10:275–281
60. Camper SA, Saunders TL, Kendall SK, Keri RA, Seasholtz AF, Gordon DF, Birkmeier TS, Keegan CE, Karolyi IJ, Roller ML, Burrows HL, Samuelson LC 1995 Implementing transgenic and embryonic stem cell technology to study gene expression, cell-cell interactions and gene function. Biol Reprod 52:246–257
61. Behringer RR, Mathews LS, Palmiter RD, Brinster RL 1988 Dwarf mice produced by genetic ablation of growth hormone-expressing cells. Genes Dev 2:453–461
62. Borrelli E, Heyman RA, Arias C, Sawchenko PE, Evans RM 1989 Transgenic mice with inducible dwarfism. Nature 339:538–541
63. Inoue K, Couch EF, Takano K, Ogawa S 1999 The structure and function of folliculo-stellate cells in the anterior pituitary gland. Arch Histol Cytol 62:205–218
64. Inoue K, Taniguchi Y, Kurosumi K 1987 Differentiation of striated muscle fibers in pituitary gland grafts transplanted beneath the kidney capsule. Arch Histol Jpn 50:567–578
65. Mogi C, Miyai S, Nishimura Y, Fukuro H, Yokoyama K, Takaki A, Inoue K 2004 Differentiation of skeletal muscle from pituitary folliculo-stellate cells and endocrine progenitor cells. Exp Cell Res 292:288–294
66. Guha U, Gomes WA, Kobayashi T, Pestell RG, Kessler JA 2002 In vivo evidence that BMP signaling is necessary for apoptosis in the mouse limb. Dev Biol 249:108–120
67. Ohuchi H, Hori Y, Yamasaki M, Harada H, Sekine K, Kato S, Itoh N 2000 FGF10 acts as a major ligand for FGF receptor 2 IIIb in mouse multi-organ development. Biochem Biophys Res Commun 277:643–649
68. De Moerlooze L, Spencer-Dene B, Revest J, Hajihosseini M, Rosewell I, Dickson C 2000 An important role for the IIIb isoform of fibroblast growth factor receptor 2 (FGFR2) in mesenchymal-epithelial signalling during mouse organogenesis. Development 127:483–492
69. Stallock J, Molyneaux K, Schaible K, Knudson CM, Wylie C 2003 The pro-apoptotic gene Bax is required for the death of ectopic primordial germ cells during their migration in the mouse embryo. Development 130: 6589–6597
70. Vyas S, Juin P, Hancock D, Suzuki Y, Takahashi R, Triller A, Evan G 2004 Differentiation dependent sensitivity to apoptogenic factors in PC12 cells. J Biol Chem 279: 30983–30993
71. Jansen BJ, van Ruissen F, Cerneus S, Cloin W, Bergers M, van Erp PE, Schalkwijk J 2003 Tumor necrosis factor related apoptosis inducing ligand triggers apoptosis in dividing but not in differentiating human epidermal keratinocytes. J Invest Dermatol 121:1433–1439
72. Parks JS, Brown MR, Baumbach L, Sanchez JC, Stanley CA, Gianella-Neto D, Wu W, Oyesiku N, Natural History and Molecular mechanisms of hypopituitarism with large sella turcica. Program of the 80th Annual Meeting of The Endocrine Society, New Orleans, LA, 1998, p 470 (Abstract P3-409)
73. Bachrach E, Li S, Perez AL, Schienda J, Liadaki K, Volinski J, Flint A, Chamberlain J, Kunkel LM 2004 Systemic delivery of human microdystrophin to regenerating mouse dystrophic muscle by muscle progenitor cells. Proc Natl Acad Sci USA 101:3581–3586

***Molecular Endocrinology* is published monthly by The Endocrine Society (http://www.endo-society.org), the foremost professional society serving the endocrine community.**